

# Microstructure instability in TiC-316L stainless steel cermets

Chenxin Jin, Kevin P. Plucknett \*

Dalhousie University, 1360 Barrington Street, Materials Engineering, Department of Process Engineering and Applied Science, B3H 4R2 Nova Scotia, Canada



## ARTICLE INFO

### Article history:

Received 21 October 2015

Received in revised form 18 March 2016

Accepted 22 March 2016

Available online 24 March 2016

### Keywords:

Titanium carbide

Stainless steels

Cermets

Core-rim structure

Scanning electron microscopy

Focused ion beam microscopy

## ABSTRACT

Titanium carbide (TiC) based cermets are commonly used in wear and corrosion resistance applications. The microstructural evolution, and related compositional instability, of TiC-based cermets prepared with a 316-L stainless steel binder is described in the present work. Samples were fabricated using a simple vacuum melt-infiltration procedure, with 5 to 30 vol.% binder. Infiltration temperatures ranged from 1475 °C to 1550 °C, held for up to 240 min, typically resulting in sintered samples with densities in excess of 99% of theoretical. It is demonstrated that irregularly shaped grains (concave/hollow) can arise after sintering, especially at 1475 °C, which is discussed in terms of the 'instability of the solid-liquid interface' theory. It is demonstrated that a complex, multi-layer core-rim structure arose for the cermets, with accommodation of selected steel constituents into the rim of the TiC grains. In particular, it is shown that the Mo in the original 316-L stainless steel is essentially fully depleted from the metallic binder phase, forming a Mo-rich inner-rim layer on the TiC grain cores.

© 2016 Elsevier Ltd. All rights reserved.

## 1. Introduction

Cermets are composite materials that combine hard, brittle ceramics with a ductile metallic binder phase. Compared with conventional 'hardmetals', such as tungsten carbide-cobalt (WC-Co), cermets are lighter in weight with high strength and toughness, combined with excellent wear and corrosion resistance [1–4]. Titanium carbide (TiC) is widely used as the ceramic component in cermets due to its high melting point (3065 °C), hardness, and wear resistance [1–4]. Conventionally, TiC based cermets are mainly used as tooling and wear resistant materials, such as cutting tools, bearings, drawing dies, etc. Depending on the metallic binder phase employed, the applications can potentially be broadened to high-stress and high-temperature environments [5]. Several studies have been conducted assessing the effects of composition and microstructure on the behaviour cermets [6–12], particularly the role of the binder volume fraction. In addition to the binder fraction, the grain size and binder mean free path are also influence the physical properties [13].

Some common examples of the metallic phase used in TiC-based cermets include Ni and Fe [14,15]. Ni is the most commonly used metallic binder in these cermets, which is mainly due to the good wetting response during liquid phase sintering, combined with the reasonable mechanical properties of Ni [2]. More recently, TiC cemented with Ni-Mo alloys have proved to be applicable in cutting tools and severe wear conditions [4]. However, due to their relatively low cost and good mechanical properties, Fe alloys are being studied and applied as cermet binders. In particular, austenitic stainless steels have relatively

high strength, which is maintained to moderately elevated temperatures, therefore offering potential for use as the binder phase in cermet systems [16–19]. This is combined with reasonable corrosion resistance when stainless steels are incorporated into a cermet structure [10].

It is well known that the addition of Mo or Mo<sub>2</sub>C reduces the binder melt wetting angle with TiC to essentially zero when using Ni-based alloys, and typically a core-rim structure is generated, which can be beneficial to the mechanical properties of the cermet [20,21]. The core is invariably the original TiC, and the rim phase is an alloy of (Ti,Mo)C [22]. There can also be different types of rims generated in other specific systems, particularly Ti(C,N) based cermets [23,24]. Oswald-ripening during the dissolution-precipitation process is invariably believed to form the core-rim structure [22–24], but diffusion of Mo into the TiC has also been suggested [25]. Similarly, Guo and colleagues examined the effects of Mo<sub>2</sub>C addition when using an Fe binder for Ti(C,N)-based cermets [26]. They demonstrated an improvement in binder wettability, due to Mo<sub>2</sub>C addition, and highlighted improved properties and the formation of a core-rim structure.

The aim of the present work was to study the effects of composition and sintering duration on the microstructure evolution of a range of TiC-316L stainless steel cermets, in order to obtain an understanding of the microstructure evolution and stability, and its potential influence on cermet properties.

## 2. Experimental procedure

### 2.1. Sample preparation

The TiC powder was obtained from Pacific Particulate Materials Ltd. (Vancouver, BC, Canada) with a quoted manufactured mean particle

\* Corresponding author.

E-mail address: [kevin.plucknett@dal.ca](mailto:kevin.plucknett@dal.ca) (K.P. Plucknett).

size of  $\sim 1.3 \mu\text{m}$ , which was confirmed through subsequent particle size analysis [27]. The TiC powder itself shows a bimodal distribution, with fine, nano-sized material ( $\sim 90\text{--}100 \text{ nm}$ ) combined with coarser particles (from  $\sim 500 \text{ nm}$  to  $\sim 2 \mu\text{m}$ ) [27]. The austenitic stainless steel powder (grade 316L), used as the binder phase, was sourced from Alfa Aesar (Ward Hill, MA, USA), with a nominal particle size of  $\sim 149 \mu\text{m}$  ( $\sim 100$  mesh). The melting response of the 316L powder was confirmed through differential scanning calorimetry (DSC; Model SDT Q600, TA Instruments, New Castle, DE, USA), heating at a rate of  $20^\circ\text{C}/\text{min}$  under a flowing Ar atmosphere. Using this approach the onset of the melting endotherm was confirmed by DSC to occur at  $\sim 1400^\circ\text{C}$ . The chemical compositions of the TiC and 316L starting powders were confirmed using inductively coupled plasma optical emission spectroscopy (ICP-OES; Model Varian Vista Pro, CA, USA), for the principle elemental species. The C content of the as-received steel powder was determined using an inert gas fusion method (Model CS-444, Leco Instruments, Mississauga, ON, Canada). The analyzed compositions of the TiC and 316L steel are presented in Tables 1 and 2, respectively.

The TiC pellets (each  $\sim 7.4 \text{ g}$  mass) were uniaxially compacted in a hardened steel die at a pressure of around  $\sim 45 \text{ MPa}$ . The samples were then vacuum-sealed and further consolidated by cold isostatic pressing (CIPing) at  $\sim 208 \text{ MPa}$ . This procedure generated TiC pellets with a green density of  $59.2 \pm 1.3\%$  of theoretical (i.e.  $\sim 40 \text{ vol.}\%$  porosity after CIPing), based on a TiC theoretical density of  $4.93 \text{ g}/\text{cm}^3$ . A simple melt-infiltration/sintering route was used to fabricate the samples, which has been discussed in detail in an earlier publication [28]. With this approach a pre-determined amount of 316-L stainless steel powder, to give nominal binder contents ranging from 5 to 30 vol.%, was placed on top of the CIPed TiC pellets, which were contained in an aluminium oxide ( $\text{Al}_2\text{O}_3$ ) crucible on a bed of bubble  $\text{Al}_2\text{O}_3$ . The samples were sintered in a graphite resistance furnace (Materials Research Furnaces, Suncook, NH, USA) at  $1475^\circ\text{C}/15 \text{ min}$  to get a fine-grained structure,  $1550^\circ\text{C}$  for 60 min to get intermediate-sized grains, and  $1550^\circ\text{C}$  for 240 min to get coarse grains. Heating and cooling rates of  $10^\circ\text{C}/\text{min}$  and  $25^\circ\text{C}/\text{min}$ , respectively, were used under a dynamic vacuum ( $\sim 20 \text{ mTorr}$ ).

## 2.2. Cermet characterization

The densities of the sintered cermets were determined using Archimedes' immersion method, in water. For microstructural characterization, the cermets were initially ground flat on both sides using a diamond peripheral wheel, and then polished to a mirror-like finish (starting from a  $125 \mu\text{m}$  diamond pad and finishing with  $0.25 \mu\text{m}$  diamond paste). The samples were examined with optical microscopy (Model BX-51, Olympus Canada, Richmond Hill, Ontario, Canada) and scanning electron microscopy (SEM; Model S-4700, Hitachi High Technologies, Tokyo, Japan). The mean carbide grain size,  $d_c$ , was determined using the linear intercept method, from the digital SEM images, with a minimum 300 TiC grains measured per sample [29]. The contiguity values of each of the samples,  $C$ , were measured by counting the numbers of carbide/carbide ( $N_{c/c}$ ) and carbide/binder ( $N_{c/b}$ ) interfaces intercepted through horizontal lines on the digitized microstructural images, and determined following [30]:

$$C = \frac{2N_{c/c}}{2N_{c/c} + N_{c/b}} \quad (1)$$

where  $N_{c/c}$  and  $N_{c/b}$  are the number of carbide-carbide and carbide-

**Table 1**

Measured composition of the as-received TiC powder using ICP-OES. Note that the C content was not determined.

TiC powder	Ti	Co	W
Conc. (wt.%)	76.80	0.23	2.22

**Table 2**

Measured composition of 316-L as-received powder (in wt.%). Elements determined using ICP-OES, except for C, which is measured using inert gas fusion.

316-L	Cr	Mo	Mn	S	Ni	Si	C	Fe
Conc. (wt.%)	16.81	2.22	0.10	0.01	13.40	0.59	0.025	64.34

binder interfaces intercepted, respectively [30]. Based on information obtained for both the carbide grain size and contiguity, the binder mean free path (MFP),  $d_b$ , was then determined following [30]:

$$d_b = \frac{1}{1-C} \left( \frac{V_b}{V_c} \right) d_c \quad (2)$$

where  $V_c$  and  $V_b$  are the volume fraction of carbide and binder. The binder MFP can be viewed as a measure of the dimensions of the metallic ligaments separating the carbide grains.

Compositional analysis of the cermets was performed in the SEM using energy-dispersive X-ray spectroscopy (EDS; Model Inca X-Max<sup>N</sup>, Oxford Instruments, Abingdon, UK). X-ray diffraction (XRD; Model Bruker D-9 Advance) was used to examine the crystalline phases present in the samples, using a Co source to minimize Fe fluorescence. To assess the sub-surface structure of specific TiC grains, a focused ion beam (FIB) microscope was used (Model 2000-A, Hitachi High Technologies, Tokyo, Japan), which utilizes Ga ions to 'micro-machine' the surface at site-specific locations.

## 3. Results and discussion

### 3.1. Basic cermet microstructure

As shown in Fig. 1, the TiC-316L stainless steel cermets sintered at  $1475^\circ\text{C}$  for 15 min (i.e. fine-grained) had achieved densities in excess of 95% of the theoretical estimates. The theoretical density was calculated using a simple rule of mixtures, based on the nominal volume fractions of the TiC and 316L stainless steel phases and their respective densities. The melt-infiltration/sintering procedure itself results in densification arising from two primary contributions, namely simple infiltration of the available porosity by the molten steel alloy and, perhaps more importantly, liquid phase sintering. In particular, when low binder contents are employed (i.e. 5 vol.%), the liquid phase sintering contribution is significant (leading to particle rearrangement, and dissolution/re-precipitation mechanisms), as pore filling alone would leave  $>30 \text{ vol.}\%$  porosity (the initial TiC preforms exhibit  $\sim 40 \text{ vol.}\%$  porosity after compaction).

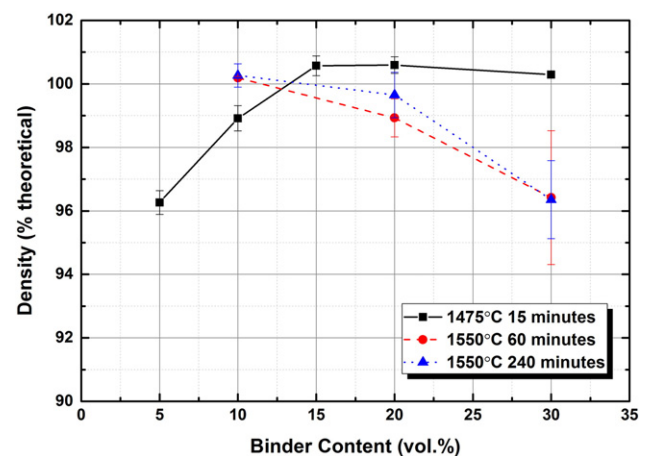


**Fig. 1.** The effects of binder content and sintering temperature on the density of the cermets.

Download English Version:

<https://daneshyari.com/en/article/1602627>

Download Persian Version:

<https://daneshyari.com/article/1602627>

[Daneshyari.com](https://daneshyari.com)